LAWRENCE
LIVERMORE
NATIONAL
LABORATORY

LLNL-JRNL-506051

Enhancement factor distributions measured for SERS nanocapsules

T. A. Laurence, G. Braun, M. Moskovits, N. Reich

October 17, 2011

Nano Letters

Disclaimer

Enhancement factor distributions measured for SERS nanocapsules

Ted A. Laurence[A], Gary Braun[B], Martin Moskovits[B], and Norbert Reich[B]*

[A]Physical and Life Sciences Directorate, Lawrence Livermore National Laboratory, Livermore, CA 94550

[B]Department of Chemistry and Biochemistry, University of California, Santa Barbara, CA 93106

**Corresponding author. E-mail: laurence2@llnl.gov.*

We characterize the distribution in SERS enhancement factors observed in hot spots of single Ag "nanocapsules" formed via controlled nanoparticle linking, polymer encapsulation, and small molecule infusion. The enhancement factors are calculated by comparing signal intensities of 4-mercaptobenzoic acid (MBA) measured from single SERS hot spots to intensities measured from high concentration aqueous solutions of MBA. That the measurements were carried out on nanoparticle dimers, each with a single, dominant hot spot is verified by showing that the strong rotational diffusion correlation amplitudes are only consistent with single hot spots possessing strong polarization sensitivity, which would be absent for nanoparticle monomers or ensembles of orientationally uncorrelated dimers. The intensity distributions determined from diffusing and fixed nanoparticles is used to determine the distribution of enhancement factors for these nanocapsules, which were found to range from 10^7 to 10^{10}.

Introduction

A current objective of many SERS studies is to obtain more highly enhancing and more uniformly enhancing SERS substrates to facilitate quantitative, analytical applications. Recently, we reported a SERS substrate (that we dubbed "SERS nanocapsules") consisting of encapsulated nanoparticle dimers as its major component, based on a controlled Ag nanoparticle linking and passivation scheme, that exhibited strong, uniform SERS signals [1-3]. Wustholz et al. have used a similar approach to obtain consistent enhancement factors (EFs) correlating nanoparticle aggregate geometry determined from electron microscopy with SERS for Au [4]. We also reported a methodology for rapidly characterizing the distribution of intensities and ratios between intensities from diffusing nanoparticles in solution [2]. More recently methodological approaches have been reported for measuring entire spectra of flowing, individual nanoparticle clusters with high signal to noise [5].

The goal of the current work is to measure the enhancement factors of hot spots of individual Ag SERS nanocapsules freely diffusing in solution, comparing these results to samples immobilized on a glass coverslip. In this study we defined enhancement along the lines of the SERS substrate enhancement factor (SSEF) suggested by Le Ru et al [6], except applied to individual SERS nanocapsules. However, we did not use the single molecule enhancement factors also proposed in Le Ru et al. Instead, we determined the average enhancement from all of the molecules adsorbed in the hotspot of a single nanocapsule. To accomplish this the nanocapsules were exposed to enough MBA to allow the molecule to saturate all of the binding sites in a given hotspot.

Materials and Methods

Nanocapsule production and loading

The nanocapsules are produced and loaded with 4-mercaptobenzoic acid (MBA) as described previously in Refs. [1-3]. Measurements of diffusing nanoparticles are performed on as-prepared solutions without dilution.

Preparation of high concentrations of MBA

Two high concentration solutions of MBA in methanol (43 mM and 600 mM) were prepared for measuring the intensity of Raman lines of MBA. The solutions were kept at 50^{o}C on a heating stage until use. The measurements were performed in < 2 minutes to avoid MBA coming out of solution. Measurements were completed before crystallization was visible.

Single nanoparticle SERS and Raman intensity fast timing experimental setup

The measurements of Raman line intensity and rotational diffusion-induced intensity fluctuation of freely diffusing nanoparticles are performed as described by Laurence et al. [2]. The Rayleigh scattering channel was eliminated for these measurements. A piezo scanning stage (LP200, MadCityLabs) was added for imaging immobilized nanoparticles. For the freely diffusing

nanoparticles, the laser was linearly polarized. For the immobilized nanoparticles, the laser was circularly polarized.

Single nanoparticle SERS and Raman spectral experimental setup

We use the system described in Talley et al [7] for measuring the Raman and SERS spectra of immobilized nanoparticles and Raman lines of bulk solutions.

Theory

Correlation amplitudes caused by rotational diffusion

To determine whether or not a signal comes from an individual hot spot, we perform autocorrelations on nanocapsules undergoing free translational and rotational diffusion. The excitation laser light is polarized, and our SERS correlation spectroscopy setup [2] allowed us to measure both the scattered component whose polarization is aligned with, and perpendicular to the polarization of the exciting light. The expected correlation amplitude due to rotational diffusion for dipolar scattering from an individual SERS hot spot was derived using a simplified mathematical framework based on the more general case described in Ehrenberg et al.[8] We calculate the expected correlation amplitudes for spherical rotors. Defining θ as the polar angle between the laser excitation and the dipole of the SERS hot spot, and ϕ as the azimuthal angle; and defining $\mu = \cos\theta$, the scattered intensity for a dipole at these angles is

$$I_{\text{scat}}(\theta,\phi) = A\cos^2\theta\left(\cos^2\theta + \sin^2\theta\cos^2\phi\right) = A\mu^2\left[\mu^2 + \left(1-\mu^2\right)\cos^2\phi\right] \tag{1}$$

For a correlation function amplitude estimate, one calculates the time evolution of intensity given that at time t=0 a scattered photon was detected. The probability distribution that a dipole scattered a photon at time t=0 is

$$P_0(\mu,\phi) = {}^{3}\!/_{4\pi}\,\mu^2 d\mu d\phi \tag{2}$$

For $t\to\infty$ $P_\infty(\mu,\phi) = {}^{1}\!/_{4\pi}\,d\mu d\phi$. The fraction of the initial correlation amplitude due to rotational diffusion is

$$A_P = \frac{\left\langle I_{\text{scat}}(t=0)\right\rangle - \left\langle I_{\text{scat}}(t\to\infty)\right\rangle}{\left\langle I_{\text{scat}}(t=0)\right\rangle} \tag{3}$$

These values can be calculated as

$$\left\langle I_{\text{scat}}(t=0)\right\rangle = \int_{-1}^{1} d\mu \int_{0}^{2\pi} d\phi P_0(\mu,\phi) I_{\text{scat}}(\mu,\phi) = A\,{}^{3}\!/_{2}\left({}^{1}\!/_{7} + {}^{1}\!/_{5}\right) \tag{4}$$

and

$$\left\langle I_{s} \quad (t_{c} = \infty) \right\rangle_{\mu} = \int_{-1}^{1} d\mu \int_{0}^{2\pi} d\phi P_{\infty}(\mu,\phi) I_{t}(\mu,\phi) = A \frac{1}{2}\left(\frac{1}{5} + \frac{1}{3}\right) \tag{5}$$

Using Eqs. (3)-(5), we obtain $A_P \approx 0.48$. This value may be compared with the values obtained in Fig. 3C. Samples with more than one hot spot per particle would have lower values of A_P.

Results and Discussion

Calibration of enhancement factors

We calibrate our measurements of enhancement factors by comparing Raman signals of MBA in solution with MBA signals from SERS nanocapsules. We performed spectroscopy to identify Raman lines on one microscope, and determined absolute signal strengths on a separate microscope setup. To determine intensities, we count photons over narrow spectral ranges defined by bandpass filters rather than acquiring entire spectra. While sacrificing spectral information, this approach dramatically increases temporal resolution, allowing measurement of rotational diffusion of particles and robust identification of the signal arising from an individual hot spot.

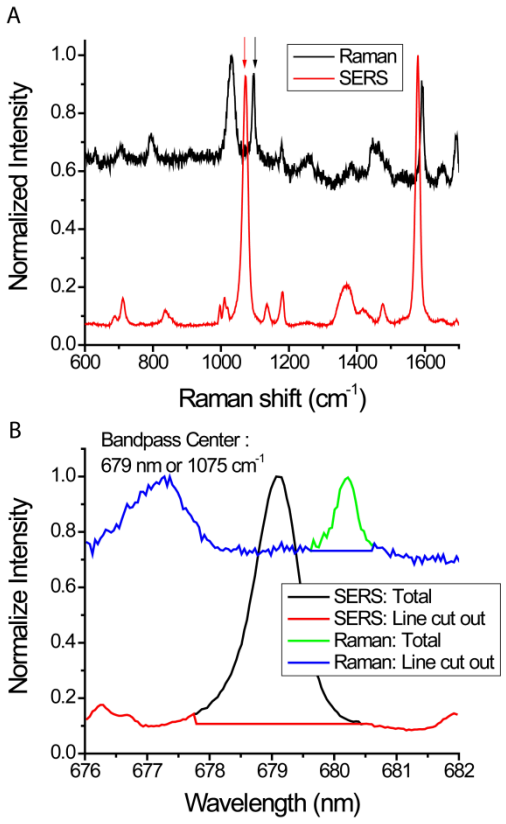

Figure 1: A. The bulk Raman spectrum of MBA in methanol and the SERS spectrum of MBA are shown. Note the small change in the Raman shift for the ring breathing mode of MBA between bulk Raman and SERS . B. The fraction of signal monitored using a 679DF6 bandpass filter from the ring-breathing mode of MBA near 1080-1100 cm^{-1} is determined from the spectra.

Raman and SERS signals in our fast-timing setups are collected using bandpass filters chosen to capture a particular Raman band. To compare samples that have spectral position and shape differences in the area of interest we determine the fraction of the signal within the filter that comes from the specific Raman line (Figure 1). We chose to measure the ring breathing mode as it is a commonly used band for SERS and is present in both the free molecule's Raman spectrum and in the SERS spectrum. The SERS peak is shifted from the free molecule (Figure 1A) and is centered within the spectral range of the bandpass filter (Figure 1B). This allows us to determine the relative Raman intensities in the fast-timing experimental setup for MBA SERS. The fraction of signal in the bandpass coming from MBA on solution is f_{Raman} =2.4%±1% and f_{SERS}=56%±15% for the fraction detected as SERS. (Since the MBA signal occurs at a fixed wavenumber with respect to the excitation frequency we can determine the background signal by exciting with a second wavelength, thereby shifting the SERS spectrum, and leaving a featureless background signal in the 850 cm^{-1} to 1000 cm^{-1} bandpass wavelength range.) In the fast-timing experimental setup we estimated the fractions by switching between a 633 nm HeNe excitation and a 640 nm diode excitation (Figure 2).

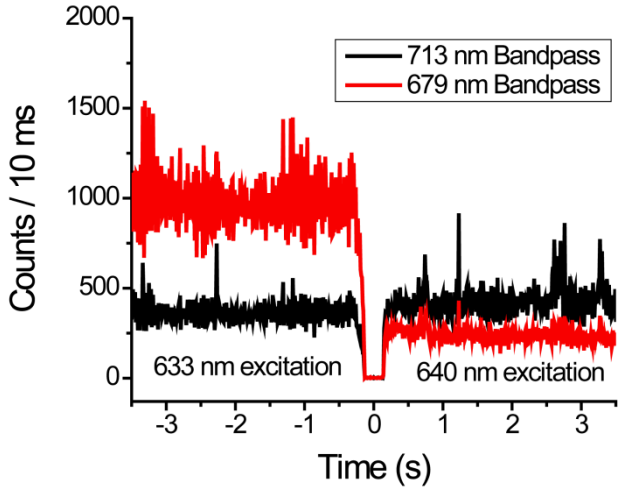

Figure 2: The laser excitation is switched by a flipper mirror at time 0 from a 633 nm HeNe laser to a 640 nm diode laser adjusted to have the same laser power (150 μW). The signal detected in the 679 nm bandpass goes down 70% due to the Raman band at 1080 cm^{-1} slipping out of the bandpass filter toward the red. The signal in the 713 nm filter is essentially unchanged since no Raman line is present for that bandpass filter.

The calibration is finalized by comparing Raman and SERS measurements at the same laser excitation rates 600 μW with a ~500 nm diameter beam. This comparison needs to take into account the number of MBA molecules excited under each condition. For the confocal Raman measurements, the 500 nm diameter beam combined with the emission pinhole were found to have an effective detection volume of 2.8±0.5 femtoliters from separate fluorescence correlation spectroscopy measurements of Alexa 647. N_{Raman}=1E9±2E8 molecules of MBA are thus present in this detection volume for a concentration of 600 mM. The total intensity of this solution was measured to be S_{Raman} = 8.2±0.1 kHz, which is corrected for the reduced fraction collected during the fast measurements of interest (2.4%). The corresponding signal strength of $S_{\mathrm{Raman}} f_{\mathrm{Raman}}$ is 200±70 Hz for the monitored Raman line.

The TEM images taken of SERS nanocapsules [eg. from Ref. [1]] provides estimates (10-30 nm diameter) for the contact area between nanoparticles. The area of contact (and presumably the hot spot area) would therefore range from 80 nm^2 to 700 nm^2. Assuming monolayer coverage of MBA on these areas [9] with a measured spacing of 0.8 x 0.8 nm, we expect 100 to 1000 MBA molecules in a given hot spot. We use the average value N_{SERS} = 550 molecules per hot spot in our calculations, with the understanding that there is approximately half an order of magnitude uncertainty in that value.

We use the foregoing observations and the following formula to calculate the SERS enhancement factor *EF*,

$$EF = \frac{f_{\mathrm{SERS}} S_{\mathrm{SERS}} I_{\mathrm{Raman}} N_{\mathrm{Raman}}}{f_{\mathrm{Raman}} S_{\mathrm{Raman}} I_{\mathrm{SERS}} N_{\mathrm{SERS}}} \tag{6}$$

I_{SERS} and I_{Raman} are the laser excitation intensities for the Raman and SERS experiments. The largest uncertainties in the values come from the estimated value used for the number of MBA molecules per SERS hot spot.

Measurement of enhancement factors for SERS nanocapsules

We calculate the enhancement factors for our nanocapsules by measuring the SERS intensity of the 1077 cm^{-1} Raman band of MBA loaded into nanocapsules. The nanocapsules are allowed to randomly diffuse through a detection volume defined by a tightly focused 633 nm excitation and confocal detection as described. The intensity of the 1077 cm^{-1} Raman band is filtered using a bandpass filter, and each scattered photon is timed with an avalanche photodiode. We are able to sample the Raman intensity of a large number of nanoparticles in this way, with the drawback that each nanoparticle can travel a different diffusive path through the confocally-defined detection volume.

SERS hot spots formed by interparticle junctions exhibit a very strong polarization response that can be monitored at the single particle level [10]. A strong polarization response strongly suggests that a single hot spot dominates the observed signal; the only alternative possibility is

that multiple hot spots are aligned by chance. By using this property, it is possible to distinguish between single hot spot signals and multi-hot spot signals by measuring polarization response.

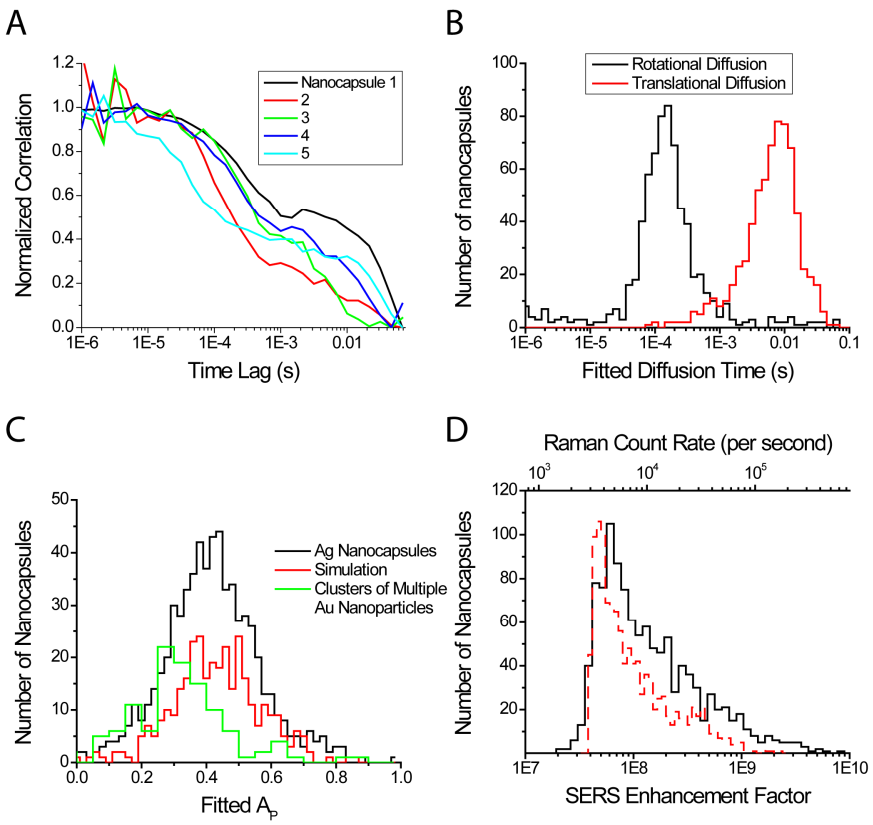

Figure 3: Determination of single hot-spot enhancement factors for diffusing nanocapsules. A. Correlation functions calculated for transits of individual nanocapsules. Rotational and translational diffusion timescales are visible. B. Fitted rotational and translational diffusion timescales for individual nanocapsules. C. Histogram of A_P, the fraction of total correlation amplitude, for measured nanocapsules (black) and simulated spherical dipole scattering centers (red) diffusing through a Gaussian detection volume. Green line shows distribution of A_P for clusters of multiple Au nanoparticles studied in Ref. [2]. D. Determined SERS enhancement factors for individual hot spots (black line). A simulation of diffusing particles with a uniform excitation response (dotted red line) is shown.

It was previously shown that the polarization sensitivity of SERS leads to rotational diffusion-induced intensity fluctuations from nanoparticles randomly diffusing in aqueous solutions [2, 11]. Correlation functions calculated on individual nanoparticles as discussed in [2, 12] show two time scales: a shorter, polarization sensitive timescale due to rotational diffusion with respect to the excitation polarization, and a longer timescale due to translational diffusion into and out of the detection volume (Fig. 3A). The timescales for each of these processes is extracted and can be used for sizing the nanocapsules (Fig. 3B). A rotational diffusion timescale of 100 μs

corresponds to a nanocapsules size a little more than 100 nm, consistent with the TEM images of dimers with polymer coating [2].

Detecting the strength of these intensity fluctuations provides a way to directly observe that a nanoparticle has a single or dominant SERS hot spot for a large number of nanoparticles. The relative magnitude of the rotational diffusion components as shown in Fig. 3C (black line, typically 40% of correlation amplitude) indicates that the SERS intensities values measured are dominated by signals from single hot spots. The distribution $A_{P,}$ the fraction of total correlation amplitude due to rotational diffusion, is very similar to that obtained from a simulation of 100 nm spherical particles which scatter preferentially along a single axis of polarization (red line, Fig. 3C). The distribution observed is in contrast to that observed for clusters of multiple Au nanoparticles studied in Ref. [2] (green line); spherically symmetric particles would show no polarization response, resulting in $A_P=0$. The simulated particles diffuse rotationally with respect to the excitation polarization axis and translationally through the confocal detection volume. The width of the distribution is expected to depend noticeably on the number of hot spots associated with a single diffusing particle. The analyzed results from our measurements are consistent with the majority of diffusing entities possessing a single hot spot. This suggests that the SERS enhancement factors extracted from Raman intensities using this method are for the individual hot spots, minimizing the typical diminution of the EF by the much weaker (isotropic) SERS originating from monomers. (Despite the enrichment of the sample in dimers, it still contains numerous monomers.) Important for synthetic optimization, this result is expected to be coincident to the EF distribution that would be obtained from a dimer product that is purified from all monomers and large aggregates, even though such a thorough purification was not carried out.

The distribution of SERS enhancement factors computed from the diffusing nanocapsules using Eq. (6) are shown in Fig. 3D. The enhancements range from ~3E7 to 1E10. The most probable value is ~ 6E7, and the ranges are consistent with previously observed values in Ag nanoparticle junctions [4, 6]. (The uncertainty in these values is approximate ±5.) However, it does appear that there is a wide distribution in the enhancement factors observed; the rapid rise in the distribution above 1E7 is due to the photon burst detection threshold. The simulation of freely diffusing particles with uniform response in a confocal detection volume (described in [13]) shown in Fig. 3D (dotted red line) suggests that the observed wider distribution is not fully explained by the burst detection procedure. We previously showed that the nanocapsules produced more consistent SERS signals than randomly aggregated Ag nanoparticles [2], but even so the enhancement factors are distributed over two to three orders of magnitude.

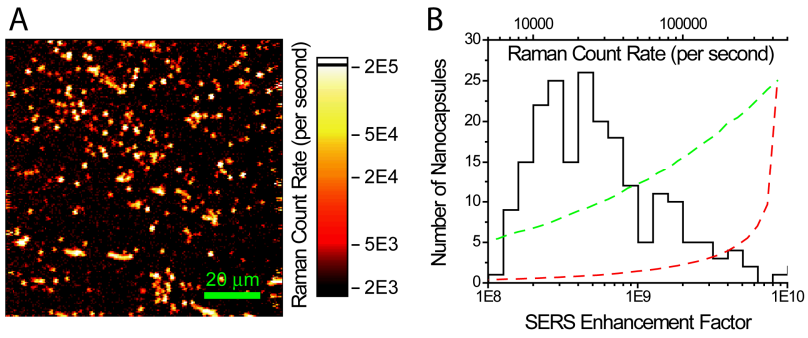

Figure 4: SERS enhancement factors for surface-immobilized nanocapsules. A. Confocal scattering image. B. Enhancement factors extracted for individual nanocapsules in A. Dotted red line is distribution expected for uniform sample with circular excitation polarization. Dotted green line is distribution expected for uniform sample with linear excitation polarization.

In the measurements on freely diffusing nanocapsules, the varying diffusion paths the nanocapsules take through the detection volume contribute to the observed intensities and the distribution of enhancement factors observed. To determine if this is a dominant source in the distribution observed, we measured enhancement factors of nanocapsules immobilized on a coverslip. As shown in Fig. 4, we again see a rather wide distribution of Enhancement factors, with a rapid rise near the detection threshold (which for this case corresponded to EF=1E8). In this experiment we used circular polarization for excitation to minimize effects of the highly polarized scattering response of the nanocapsules. However, we were not able to eliminate the possibility of alignment along the optical axis. If α is the angle of the dimer polarization with respect to the optical axis, the observed intensity depends on $\sin^4 \alpha$. A simple simulation based on this (dotted red line) shows a distribution very different from the observed distribution. This result does not depend on having perfect circular polarization: linear excitation polarization (dotted green line) still produces a distribution very different from the observed distribution. The conclusion is that the contribution of diffusion paths or polarization orientations does not dominate the distribution in SERS enhancement factors.

Conclusion

We have measured the SERS enhancement factors of SERS nanocapsules to vary from ~1E7 to ~1E10, consistent with values previously determined in nanoparticle junctions. Large-scale rotational diffusion was used to verify that the measurements were carried out on individual hot spots. Nanocapsules diffuse into and out of a confocal detection volume allowing these measurements to be performed quickly, obtaining measurements on more than a thousand nanocapsules per 10 minute acquisition time. These results show that the intense (hot spot) fraction of a SERS-active mixture can be quantified by relative EF distribution. The hot spot polarization sensitivity may be used as a quick way of determining the enhancing properties of newly synthesized nanoparticle-bases SERS substrates.

Acknowledgments

This work performed under the auspices of the U.S. Department of Energy by Lawrence Livermore National Laboratory under Contract DE-AC52-07NA27344. One of us (MM) acknowledges support by the Institute for Collaborative Biotechnologies through grant DAAD19-03-D- 0004 from the U.S. Army Research Office.

References

1. Braun, G.B., S.J. Lee, T. Laurence, N. Fera, L. Fabris, G.C. Bazan, M. Moskovits, and N.O. Reich, *Generalized Approach to SERS-Active Nanomaterials via Controlled Nanoparticle Linking, Polymer Encapsulation, and Small-Molecule Infusion.* The Journal of Physical Chemistry C, 2009. **113**(31): p. 13622.
2. Laurence, T.A., G. Braun, C. Talley, A. Schwartzberg, M. Moskovits, N. Reich, and T. Huser, *Rapid, Solution-Based Characterization of Optimized SERS Nanoparticle Substrates.* Journal of the American Chemical Society, 2009. **131**(1): p. 162-169.
3. Pallaoro, A., G.B. Braun, N.O. Reich, and M. Moskovits, *Mapping Local pH in Live Cells Using Encapsulated Fluorescent SERS Nanotags.* Small, 2010. **6**(5): p. 618-622.
4. Wustholz, K.L., A.I. Henry, J.M. McMahon, R.G. Freeman, N. Valley, M.E. Piotti, M.J. Natan, G.C. Schatz, and R.P. Van Duyne, *Structure-Activity Relationships in Gold Nanoparticle Dimers and Trimers for Surface-Enhanced Raman Spectroscopy.* Journal Of The American Chemical Society, 2010. **132**(31): p. 10903-10910.
5. Goddard, G., L.O. Brown, R. Habbersett, C.I. Brady, J.C. Martin, S.W. Graves, J.P. Freyer, and S.K. Doorn, *High-Resolution Spectral Analysis of Individual SERS-Active Nanoparticles in Flow.* Journal Of The American Chemical Society, 2010. **132**(17): p. 6081-6090.
6. Le Ru, E.C., E. Blackie, M. Meyer, and P.G. Etchegoin, *Surface enhanced Raman scattering enhancement factors: a comprehensive study.* Journal Of Physical Chemistry C, 2007. **111**(37): p. 13794-13803.
7. Talley, C.E., L. Jusinski, C.W. Hollars, S.M. Lane, and T. Huser, *Intracellular pH sensors based on surface-enhanced raman scattering.* Anal Chem, 2004. **76**(23): p. 7064-8.
8. Ehrenberg, M. and R. Rigler, *Rotational Brownian motion and fluorescence intensity fluctuations.* Chemical Physics, 1974. **4**(3): p. 390-401.
9. Schafer, A.H., C. Seidel, L.F. Chi, and H. Fuchs, *STM investigations of thiol self-assembled monolayers.* Advanced Materials, 1998. **10**(11): p. 839-+.
10. Jiang, J., K. Bosnick, M. Maillard, and L. Brus, *Single Molecule Raman Spectroscopy at the Junctions of Large Ag Nanocrystals.* J. Phys. Chem. B, 2003. **107**(37): p. 9964-9972.
11. Eggeling, C., J. Schaffer, C.A.M. Seidel, J. Korte, G. Brehm, S. Schneider, and W. Schrof, *Homogeneity, Transport, and Signal Properties of Single Ag Particles Studied by Single-Molecule Surface-Enhanced Resonance Raman Scattering.* J. Phys. Chem. A, 2001. **105**(15): p. 3673-3679.
12. Laurence, T.A., Y. Kwon, E. Yin, C.W. Hollars, J.A. Camarero, and D. Barsky, *Correlation Spectroscopy of Minor Fluorescent Species: Signal Purification and Distribution Analysis.* Biophys. J., 2007. **92**(6): p. 2184-2198.

13. Laurence, T.A., A.N. Kapanidis, X.X. Kong, D.S. Chemla, and S. Weiss, *Photon arrival-time interval distribution (PAID): A novel tool for analyzing molecular interactions.* Journal of Physical Chemistry B, 2004. **108**(9): p. 3051-3067.